

Large thermoelectric figure of merit at high temperature in Czochralski-grown clathrate $\text{Ba}_8\text{Ga}_{16}\text{Ge}_{30}$

A. Saramat,^{a),b)} G. Svensson, and A. E. C. Palmqvist^{a),c)}

Department of Chemical and Biological Engineering, Chalmers University of Technology, SE-412 96 Göteborg, Sweden

C. Stiewe, E. Mueller, and D. Platzek

German Aerospace Centre (DLR), Institute of Materials Research, Linder Hoehe 51147 Cologne, Germany

S. G. K. Williams and D. M. Rowe

NEDO Centre for Thermoelectric Engineering, University of Cardiff, Newport Road Cardiff CF24 3TF, United Kingdom

J. D. Bryan and G. D. Stucky

Department of Chemistry and Biochemistry 9510, University of California, Santa Barbara, California 93106-9510

(Received 15 July 2005; accepted 2 December 2005; published online 25 January 2006)

The Czochralski method was used to grow a 46-mm-long crystal of the $\text{Ba}_8\text{Ga}_{16}\text{Ge}_{30}$ clathrate, which was cut into disks that were evaluated for thermoelectric performance. The Seebeck coefficient and electrical and thermal conductivities all showed evidence of a transition from extrinsic to intrinsic behavior in the range of 600–900 K. The corresponding figure of merit (ZT) was found to be a record high of 1.35 at 900 K and with an extrapolated maximum of 1.63 at 1100 K. This makes the $\text{Ba}_8\text{Ga}_{16}\text{Ge}_{30}$ clathrate an exceptionally strong candidate for medium and high-temperature thermoelectric applications. © 2006 American Institute of Physics.

[DOI: 10.1063/1.2163979]

I. INTRODUCTION

Efficient thermoelectric (TE) materials are characterized by a high Seebeck coefficient (S) and a comparably high electrical conductivity (σ) combined with a low thermal conductivity (λ), which results in a high TE figure of merit ($ZT = TS^2\sigma/\lambda$, where T is the absolute temperature). Recently there has been significant progress in the area of TE materials development. Promising classes of TE materials are skutterudites such as $\text{CeFe}_4\text{Sb}_{12}$ (Ref. 1) and $\text{Yb}_{0.2}\text{Co}_4\text{Sb}_{12}$,² antimonides such as Zn_4Sb_3 (Ref. 3) and half-Heusler alloys,⁴ and tellurides such as Tl_2SnTe_5 ,⁵ Tl_9BiTe_6 ,⁶ pentatellurides,⁷ and $\text{La}_{3-x}\text{Te}_4$, with $0 < x < 1/3$.⁸ Recently Hsu *et al.* showed that $\text{AgPb}_{18}\text{SbTe}_{20}$ has a ZT of 2.2 at 800 K.⁹ In addition, artificial superlattice thin-film structures of $\text{Bi}_2\text{Te}_3/\text{Sb}_2\text{Te}_3$ grown using metal-organic chemical-vapor deposition¹⁰ (MOCVD) have shown exceptionally high ZT of ~ 2.4 at 300 K, while molecular-beam-epitaxy¹¹ (MBE)-grown superlattices of $\text{PbSb}_{0.98}\text{Te}_{0.02}/\text{PbTe}$ have shown a ZT of 2.0 at 550 K.

Clathrates have received much attention as potential high-performance TE materials^{12–26} and are discussed within the framework of the “phonon-glass, electron-crystal” (PGEC) concept.²⁷ The search for high-performance TE materials in the high-temperature region (above 800 K) has led to promising results for the germanium-based clathrates.^{14,16,26}

The majority of work on clathrates has focused on group

IV based compounds with the type I structure (isostructural with the gas-hydrate clathrates), and their importance has increased since the discovery of their potential use in TE devices.²⁵ For alkaline-earth metal guests, the composition of these clathrates can be represented by $X_8Y_{16}Z_{30}$ ($X = \text{Ca, Sr, and Ba}$, $Y = \text{Al, Ga, and In}$, and $Z = \text{Si, Ge, and Sn}$), where the $\text{Ba}_8\text{Ga}_{16}\text{Ge}_{30}$ clathrate has shown especially high ZT values at temperatures above 800 K.^{14,16,26} An important issue of clathrates to address is the reproducibility of their TE properties,¹⁵ which is a key factor in the development of TE devices. The wide distribution of TE properties of germanium-based clathrates reported is likely due to differences incurred by the various synthetic procedures used to prepare them.^{15,17,24,26} Recent theoretical and experimental studies^{12,13,17–23,28,29} have recognized the Ga/Ge molar ratio of the $\text{Ba}_8\text{Ga}_{16}\text{Ge}_{30}$ compound to be a key parameter for explaining the large variability in TE properties found in the literature for this compound.^{13,16,29}

The Czochralski method is a well-known technique for controlling crystallization rates, phase purity, and composition during growth of congruently melting solids,^{30,31} and is used to deliver consistently homogenous and reproducible silicon for the semiconductor industry. Establishing reproducible synthesis parameters for the growth of the $\text{Ba}_8\text{Ga}_{16}\text{Ge}_{30}$ compound using the Czochralski technique would pave the way for possible large-scale production and use of this class of promising TE materials. For this method to work the compound must melt congruently, meaning that if it is heated above its melting point and cooled down below the melting point, it reforms. According to the literature, there exists a very narrow phase width or nonstoichiometry

^{a)} Authors to whom correspondence should be addressed.

^{b)} Electronic mail: saramat@chalmers.se

^{c)} Electronic mail: adde@chalmers.se

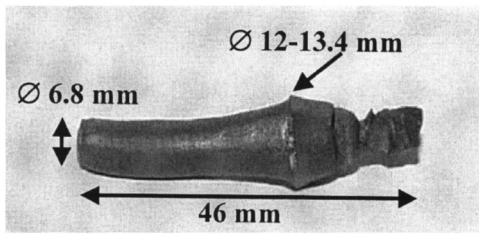


FIG. 1. Photograph of a $\text{Ba}_8\text{Ga}_{16}\text{Ge}_{30}$ crystal grown using the Czochralski method and subsequently analyzed for thermoelectric performance.

region for $M_8\text{Ga}_{16}\text{Ge}_{30}$ ($M=\text{Ba}$ and Sr) clathrates.^{15,32} Here we have used the Czochralski technique for the growth of a large crystal of the $\text{Ba}_8\text{Ga}_{16}\text{Ge}_{30}$ clathrate. The crystal was cut into disks along its length and the TE performance of these disks was evaluated up to 1000 K showing a record high ZT at temperature above 800 K.

II. MATERIALS AND METHODS

A. Sample preparation and processing

A batch of 70 g $\text{Ba}_8\text{Ga}_{16}\text{Ge}_{30}$ powder was prepared according to a previously described method^{15,29} and placed in a 20 ml EK90 graphite crucible manufactured by Ringsdorff-Werke GmbH. The crucible was placed in a materials preparation and crystal growth system [(MPCGS)-Crystalox Ltd.] at the Department of Chemical and Biological Engineering at Chalmers University of Technology. The atmosphere of the MPCGS chamber was flushed with high-purity argon four times before the temperature was raised to the melting point of $\text{Ba}_8\text{Ga}_{16}\text{Ge}_{30}$. A 7–13 mm in diameter and 46-mm-long $\text{Ba}_8\text{Ga}_{16}\text{Ge}_{30}$ crystal, shown in Fig. 1, was pulled from the melt using the Czochralski method. After cooling to room temperature, the crystal was embedded in an epoxy polymer resin (Struers), and cut into 18 disks with a thickness of approximately 1.5 mm using a diamond saw (South Bay Technology Inc, Model 660). In the following, disk 18 refers to the disk closest to the pulling rod, while disk 1 is furthest away from the rod.

B. Thermoelectric evaluations

The TE properties of the disks were evaluated as a function of temperature both at the German Aerospace Center, Cologne, Germany (DLR), and at the Centre for Thermoelectric Engineering, Cardiff, UK (NEDO). A round-robin test program to standardize the measurements between these two laboratories has previously established excellent reproducibility.³³ At DLR, an in-house built apparatus³⁴ was used for measuring S (on bar-shaped samples cut out of disks 5, 15, and 16) and σ on disk 15 within a temperature range of 300–1066 K. The specific-heat capacity (c_p) was measured at DLR using a differential scanning calorimeter (NETZSCH DSC 404). At NEDO, measurements of S on disks 1, 4, 6, 7, 9, and 18 and σ on disk 18 were performed over a temperature range of 300–900 K. The NEDO apparatus utilizes an alpha-sigma (α - σ) probe, previously described in detail elsewhere.³⁵ Thermal diffusivity (D_{th}) was measured at NEDO between front and back surfaces of the disk sample using the laser flash technique,³⁵ at nine equidistant tempera-

TABLE I. Elemental composition of n -type $\text{Ba}_8\text{Ga}_{16}\text{Ge}_{30}$ disks. The quantitative relative error using the (EPMA) can in this case be estimated to be approximately 2%. The estimation is based upon knowledge of the instrumental conditions and quantifications made on material with known compositions. When comparing the result from the different samples the significance should be considered based upon the standard deviation (given in parenthesis below the values) of the ten analytical points from each sample.

Disk No.	Ba	Ga	Ge	(Ba/Ga) _{at}	(Ba/Ge) _{at}	(Ga/Ge) _{at}
3 ^a	8.00 (0.044)	15.16 (0.082)	30.20 (0.100)	0.5277	0.2649	0.5020
10 ^a	8.00 (0.039)	15.29 (0.083)	30.20 (0.072)	0.5232	0.2649	0.5063
15 ^a	8.00 (0.045)	15.31 (0.047)	30.48 (0.056)	0.5225	0.2625	0.5023
16 ^b	7.99 (0.048)	15.37 (0.065)	30.63 (0.055)	0.5198	0.2609	0.5018
18 ^b	7.94 (0.052)	15.33 (0.045)	30.67 (0.069)	0.5179	0.2589	0.4998

^aNormalized so that Ba=8.00.

^bNormalized so that Ga+Ge=46.00.

tures within the temperature range of 400–1200 K. The total λ was calculated using the relationship between D_{th} , c_p , and the density (ρ) of the material, given in Eq. (1).

$$\lambda = \rho c_p D_{\text{th}} \quad (1)$$

The value of the density used in Eq. (1) was calculated from measurements, at room temperature, of volume and weight of a small cube cut out from the disk sample. The volume of the cube was measured using a micrometer.

The elemental composition of the selected sample disks was analyzed by electron probe micro analyzer (EPMA) using a JEOL JXA-8600 apparatus. To relate the measured intensity ratio to the concentration of the elements x-ray absorption, secondary fluorescence, electron backscattering, and the electron stopping power need to be taken into account. This was done using the conventional (ZAF) method, which uses fundamental factors to correct for the effects of atomic number (Z), absorption (A), and fluorescence (F). The data obtained from the measurements were correlated to the standard references [BaTiO_3 , elemental Ge (>99%), and GaAs (>99%)] using a ZAF-based correction method called (PRZ).³⁶

III. RESULTS AND DISCUSSION

A. Sample preparation and characterization

Figure 1 shows the $\text{Ba}_8\text{Ga}_{16}\text{Ge}_{30}$ crystal grown using the Czochralski method and analyzed for TE performance. The crystal was rod shaped (slightly faceted) with a varying diameter of 7–13 mm, a length of 46 mm, and a weight of 11.49 g. The sample density at room temperature was more than 99% of the theoretical density indicating a low degree of voids and grain boundaries in the crystal. The crystal structure of the powder collected from the cuttings agreed well with that of the $\text{Ba}_8\text{Ga}_{16}\text{Ge}_{30}$ structure previously reported.³² The normalized elemental composition of selected disk samples, cut from the large crystal, is summarized in Table I. The samples contained a lower Ga/Ge ratio

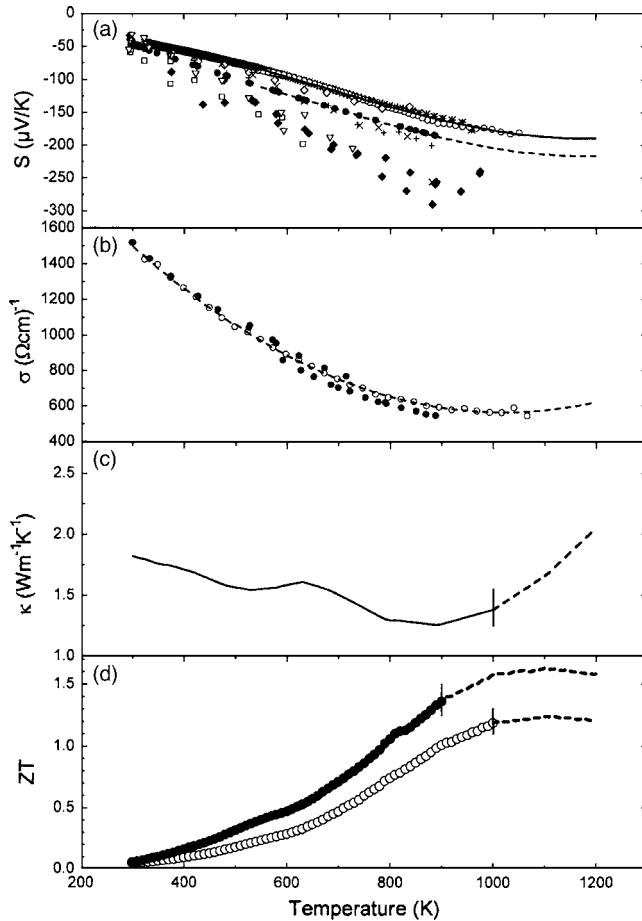


FIG. 2. (a) Seebeck coefficient (S) as a function of temperature for disks 1 (\diamond), 4 (\square), 5 (\blacklozenge), 6 (∇), 7 (\times), 9 ($+$), 15 (\circ), 16 ($*$), and disk 18 (\bullet) cut from the large $\text{Ba}_8\text{Ga}_{16}\text{Ge}_{30}$ clathrate crystal. The lines are fits and extrapolations to experimental values for disks 15 (—) and 18 (---). (b) Electrical conductivity (σ) as a function of temperature for disk 15 (\circ), its fit and extrapolation up to 1200 K (---), and disk 18 (\bullet). (c) Total thermal conductivity (κ) as a function of temperature for disk 18 and its extrapolation up to 1200 K (---). (d) Figure of merit (ZT) as a function of temperature for disk 15 (\circ) and disk 18 (\bullet), and their extrapolation up to 1200 K (---).

and a higher Ba/Ga ratio than suggested from the idealized 8:16:30 composition in agreement with previous reports for n -type samples of this material.^{16,29} The composition of the crystal varied only slightly along the pulling axis possibly being somewhat richer in Ga in the middle of the crystal, and with a small, but continuous increase in $(\text{Ba}/\text{Ga})_{\text{at}}$ ratio along the growth direction of the crystal.

B. Electrical transport measurements

The results from the temperature-dependent S measurements are shown between 300 and 1050 K in Fig. 2(a) for a number of disks originating from different parts throughout the entire length of the grown crystal. All measured disk samples showed to be n -type with values of S ranging from -42 to -50 $\mu\text{V}/\text{K}$, at room temperature. The absolute values of S increased with temperature and there was a noticeable variation in the slope of the curves between the different disks with increasing temperature resulting in a larger spread of S , from -150 to -300 $\mu\text{V}/\text{K}$ at 900 K for the samples measured. The S curves of disks originating close to the two

ends of the crystal appeared to be quite similar, whereas those from disks originating from the middle of the crystal were larger in magnitude.

For $\text{Ba}_8\text{Ga}_{16}\text{Ge}_{30}$ Sales *et al.* reported a S value of -50 $\mu\text{V}/\text{K}$ at 300 K for a single-crystal sample,¹⁷ while Bryan *et al.* reported S between -20 and -40 $\mu\text{V}/\text{K}$ at 300 K, and -35 and -60 $\mu\text{V}/\text{K}$ at 400 K for zone-refined samples.²⁹ Only a few TE characterization measurements have been made at temperatures above 400 K.^{14,16,26} Kuznetsov *et al.* reported a S of -66 $\mu\text{V}/\text{K}$ (300 K) for a polycrystalline sample and with a maximum magnitude of -194 $\mu\text{V}/\text{K}$ at 740 K.²⁶ Anno *et al.* found S to be highly dependent on x in $\text{Ba}_8\text{Ga}_x\text{Ge}_{46-x}$ with negative values for $x = 12-16$ and positive values for $x = 17-20$.¹⁶ The Czochralski-grown samples reported here exhibit x values between 15 and 16 (Table I), and the temperature-dependent S values obtained [Fig. 2(a)] fall within the range of those previously reported for n -type samples. In particular, disks 1, 15, 16, and 18 showed temperature-dependent S values between those with $x=14$ and 15 reported by Anno *et al.*¹⁶ while disks 4, 5, and 6 had S values between those with $x = 15$ and 16. This agrees with the observed increase in $(\text{Ga}/\text{Ge})_{\text{at}}$ ratio in the middle of the grown crystal. Temperature-dependent σ measurements could only be performed on two disks (15 and 18) due to size limitations of the equipment and were done in the temperature range from 300 to 1070 K, as shown in Fig. 2(b). The observed values of σ were in agreement with earlier reports.^{16,17,26,29} The two disks had very similar conductivity values across the whole temperature range, though disk 15 exhibited a smaller scatter of the data than disk 18. For disk 15 the data were measured up to 1066 K and above this temperature the curve is extrapolated using a second-order polynomial up to 1200 K. The values obtained for disks 15 and 18 were between those of the samples having $x=14$ and 15, presented by Anno *et al.*¹⁶ At first sight of Fig. 2(a) an extrapolation of S using a straight line for disks 15 and 18 may seem most suitable, but there are several hints towards a maximum absolute value of S between 1100 and 1200 K for these samples. For instance, a plateau was observed for σ at the highest measured temperature [Fig. 2(b)] interpreted as the beginning of a transition from extrinsic to intrinsic semiconducting behavior. For this reason the extrapolation in Fig. 2(b) was done to larger values of σ at higher temperatures. In Fig. 2(a), the curvature of S itself was small but pointed towards a maximum in $|S|$ at higher temperatures. Near 700 K in Fig. 2(a), d^2S/dT^2 changes sign due to an increasing contribution from minority charge carriers (holes). This change in sign of d^2S/dT^2 strongly supports the existence of a maximum in the absolute value of S at higher temperatures. The data shown in Fig. 2(a) for disks 15 and 18 were extrapolated to higher temperatures using a third-order polynomial. The maximum in $|S|$ correlates with a minimum in σ appearing around 1000 K. The reason for this minimum to appear at a lower temperature than the maximum in $|S|$ is because the second derivative of σ was positive already in the extrinsic low-temperature region; while for S it had to change sign to reach a maximum. Measurements with varying temperature (from low temperature to high temperature and vice versa) have been re-

peated several times, leading to the same results, thus showing an impressive chemical and physical stability of the $\text{Ba}_8\text{Ga}_{16}\text{Ge}_{30}$ clathrate.

C. Thermal conductivity

By measuring c_p , ρ , and D_{th} of the samples and using Eq. (1), λ was calculated. Since none of the disks satisfied the size restrictions for c_p measurements, disks 10, 15, and 16 were ground and pressed to one single disk, which was used for the c_p measurement. For D_{th} a linear extrapolation was used for the calculation of λ (and c_p was assumed to be constant above 1000 K). The resulting λ is given in Fig. 2(c), showing that λ was approximately 1.8 W/m K at room temperature and 1.25 W/m K at 900 K. Above 900 K, λ increased up to 1200 K where it was estimated to be 2.10 W/m K. The room-temperature value agrees well with previous reports on low λ for n -type $\text{Ba}_8\text{Ga}_{16}\text{Ge}_{30}$,^{16,17,29,37} as does the small temperature dependence between 300 and 900 K.¹⁶ Several recent papers have been devoted to elucidating the underlying mechanisms for the low λ of the $\text{Ba}_8\text{Ga}_{16}\text{Ge}_{30}$ clathrates.^{16,17,19,22,29,37} However, the increase in λ above 900 K has not previously been reported or discussed. These temperature-dependent λ data reveal the strongest evidence for the extrinsic to intrinsic transition. Below 900 K, λ decreased with increasing temperature due to increasing phonon-phonon scattering (Umklapp processes). The electrical contribution to λ was not affected in this extrinsic region since the charge-carrier density remained nearly constant here. At the temperature around the minimum in λ there is strong evidence for bipolar heat conduction.⁸ This means that the minority charge carriers began to affect the transport by carrying heat in the same direction as the majority charge carriers resulting in an increase of λ above 900 K. In the case of σ , however, the contribution of the minority charge carriers is cancelled by the contribution of the majority charge carriers, and hence the electrical conductivity shown in Fig. 2(b) is not changed significantly at temperatures above 900 K.

D. Figure of merit

The dimensionless ZT of disks 15 and 18 was calculated assuming that λ was the same for both samples, and the obtained values are shown in Fig. 2(d). Furthermore, all fits (for S , σ , and λ) were done in the range of existing measurement data. Disk 15 had a maximum measured ZT of 1.24 at 1000 K, while disk 18 showed a record high ZT of 1.35 at 900 K. Using the extrapolated values for S , σ , and λ the value for ZT reaches a maximum around 1100 K for both disks and becomes 1.25 and 1.63, respectively. The observed differences in ZT between these disks originate from the difference in S rather than σ , which seems to be less affected than S by small variations in the elemental composition (Table I).

These values indicate that the optimum value of x in $\text{Ba}_8\text{Ga}_x\text{Ge}_{46-x}$ for the n type is somewhere between 15 and 16, and that the large crystal grown using the Czochralski method has improved TE performance compared with previous reports on powders. Taking into account recent theoretic

cal calculations¹² and experiments¹⁶ suggesting that p -type $\text{Ba}_8\text{Ga}_{16}\text{Ge}_{30}$ clathrates give even higher ZT values than n -type, continued research on controlled crystal growth of clathrates is strongly encouraged.

IV. CONCLUSIONS

A 46 mm long and 7–13 mm in diameter crystal of the clathrate $\text{Ba}_8\text{Ga}_{16}\text{Ge}_{30}$ could successfully be grown as an n -type specimen using the Czochralski method. The atomic ratio of $(\text{Ga}/\text{Ge})_{\text{at}}$ was lower than the idealized 16:30 and found to be only slightly changing throughout the length of the crystal with a somewhat higher value in the middle of the crystal. Disk samples cut from the crystal were found to have an S ranging from approximately $-45 \mu\text{V}/\text{K}$ at 300 K to between -150 and $-300 \mu\text{V}/\text{K}$ at 900 K. With increasing temperature σ decreased gradually from 1500 to $600 (\Omega \text{ cm})^{-1}$ at 300 and 1066 K, respectively. Whereas, λ was found to be close to 1.8 W/m K at room temperature and slightly decreasing with increasing temperature to 1.25 at 900 K, above which it was found to increase rapidly. Combining these results, the dimensionless ZT for one disk was found to increase from ZT=0.08 at room temperature to ZT=1.35 at 900 K without passing through a maximum. Furthermore, temperature-dependent measurements of S , σ , and λ all showed evidence of a transition from extrinsic to intrinsic semiconductor behavior with increasing temperature suggesting an extrapolated maximum in ZT=1.63 around 1100 K. Achievement of these high ZT values with a crystal that was grown using an industrial growth method is of great importance for high-temperature TE applications such as power generation.

ACKNOWLEDGMENTS

This work was supported by the European Community under Contract No. G5RD-CT2000-00292, NanoThermel project. We direct our gratitude to the other partners in this project: M. Muhammed, M. Toprak, Y. Zang, and K. Billqvist, Royal Institute of Technology, Stockholm, Sweden, B.B. Iversen and M. Christiansen, University of Aarhus, Denmark, C. Gatti and L. Bertini, Istituto di Scienze e Tecnologie Molecolari, Milano, Italy, L. Holmgren, Termo-Gen AB, Lärbro, Sweden, and G. Noriega, Cidete Ingenieros S. L., Barcelona, Spain.

¹B. C. Sales, D. Mandrus, and R. K. Williams, *Science* **272**, 1325 (1996).

²G. S. Nolas, M. Kaeser, R. T. Littleton, and T. M. Tritt, *Appl. Phys. Lett.* **77**, 1855 (2000).

³T. Caillat, J. P. Fleurial, and A. Borshchevsky, *J. Phys. Chem. Solids* **58**, 1119 (1997).

⁴S. J. Poon, *Semicond. Semimetals* **70**, 37 (2001).

⁵J. W. Sharp, B. C. Sales, D. G. Mandrus, and B. C. Chakoumakos, *Appl. Phys. Lett.* **74**, 3794 (1999).

⁶B. Wölfing, C. Kloc, J. Teubner, and E. Bucher, *Phys. Rev. Lett.* **86**, 4350 (2001).

⁷T. M. Tritt and R. T. Littleton, *Semicond. Semimetals* **70**, 179 (2001).

⁸C. M. Bhandari, in *CRC Handbook of Thermoelectric*, edited by D. M. Rowe (CRC, Boca Raton, 1995), p. 30.

⁹K. F. Hsu *et al.*, *Science* **303**, 818 (2004).

¹⁰R. Venkatasubramanian, E. Siivola, T. Colpitts, and B. O'Quinn, *Nature (London)* **413**, 597 (2001).

¹¹T. C. Harman, P. J. Taylor, D. L. Spears, and M. P. Walsh, *Proceedings of the 18th International Conference Thermoelectrics, Baltimore, MD, 1999*

- (IEEE, New York, 1999), pp. 280–284.
- ¹²G. K. H. Madsen, K. Schwarz, P. Blaha, and D. J. Singh, *Phys. Rev. B* **68**, 125212 (2003).
- ¹³C. Gatti, L. Bartini, N. P. Blake, and B. B. Iversen, *Chem.-Eur. J.* **9**, 4556 (2003).
- ¹⁴L. Bertini *et al.*, *Proceedings of the 22nd International Conference Thermoelectrics, La Grande Motte, France, 2003* (IEEE, New York, 2003), pp. 127–130.
- ¹⁵J. D. Bryan, Dissertation Thesis, University of California at Santa Barbara, 2002.
- ¹⁶H. Anno, M. Hokazono, M. Kawamura, J. Nagao, and K. Matsubara, *Proceedings of the 21st International Conference on Thermoelectrics, Long Beach, CA, 2002* (IEEE, New York, 2002), pp. 77–80.
- ¹⁷B. C. Sales, B. C. Chakoumakos, R. Jin, J. R. Thompson, and D. Mandrus, *Phys. Rev. B* **63**, 245113 (2001).
- ¹⁸S. Paschen, W. Carrillo-Cabrera, A. Bentien, V. H. Tran, M. Baenitz, Y. Grin, and F. Steglich, *Phys. Rev. B* **64**, 214404 (2001).
- ¹⁹N. P. Blake, J. D. Bryan, S. Lattner, L. Möllnitz, G. D. Stucky, and H. Metiu, *J. Chem. Phys.* **114**, 10063 (2001).
- ²⁰N. Blake, S. Lattner, J. D. Bryan, G. D. Stucky, and H. Metiu, *J. Chem. Phys.* **115**, 8060 (2001).
- ²¹A. E. C. Palmqvist, B. B. Iversen, J. D. Bryan, S. Lattner, and G. D. Stucky, *Proceedings of the 19th International Conference on Thermoelectrics, Cardiff, UK, 2000* (IEEE, New York, 2000), pp. 113–116.
- ²²V. Keppens, B. C. Sales, D. Mandrus, B. C. Chakoumakos, and C. Laermans, *Philos. Mag. Lett.* **80**, 807 (2000).
- ²³A. Bentien, A. E. C. Palmqvist, J. D. Bryan, S. Lattner, G. D. Stucky, L. Furenlid, and B. B. Iversen, *Angew. Chem., Int. Ed.* **112**, 3759 (2000).
- ²⁴G. S. Nolas, G. A. Slack, J. L. Cohn, and S. B. Schujman, *Proceedings of the 17th International Conference on Thermoelectrics, Nagoya, Japan, 1998* (IEEE, New York, 1998), pp. 294–297.
- ²⁵G. S. Nolas, J. L. Cohn, G. A. Slack, and S. B. Schujman, *Appl. Phys. Lett.* **73**, 178 (1998).
- ²⁶V. L. Kuznetsov, L. A. Kuznetsova, A. E. Kaliazin, and D. M. Rowe, *J. Appl. Phys.* **87**, 7871 (2000).
- ²⁷G. A. Slack, in *CRC Handbook of Thermoelectrics*, edited by D. M. Rowe (CRC, Boca Raton, 1995), pp. 407–440.
- ²⁸B. C. Chakoumakos, B. C. Sales, D. G. Mandrus, and G. S. Nolas, *J. Alloys Compd.* **296**, 80 (2000).
- ²⁹J. D. Bryan, N. P. Blake, H. Metiu, G. D. Stucky, B. B. Iversen, R. D. Poulsen, and A. Bentien, *J. Appl. Phys.* **92**, 7281 (2002); **93**, 4343(E) (2003).
- ³⁰A. A. Chernov, *Modern Crystallography III* (Springer-Verlag, Berlin, 1984), Vol. 3, pp. 424–429.
- ³¹R. H. Doremus, B. W. Roberts, and D. Turnbull, *Growth and Perfection of Crystals* (Wiley, New York, 1958).
- ³²B. Eisenmann, H. Schäfer, and R. Zagler, *J. Less-Common Met.* **118**, 43 (1986).
- ³³L. Bertini *et al.*, *Proceedings of the 22nd International Conference Thermoelectrics, La Grande Motte, France, 2003* (IEEE, New York, 2003), pp. 532–536.
- ³⁴L. Bertini *et al.*, *J. Appl. Phys.* **93**, 438 (2003).
- ³⁵S. G. K. Williams, D. M. Rowe, V. Kuznetsov, and G. Min, *Proceedings of the Sixth European Workshop, Freiburg, Germany, 2001* (IEEE, New York, 2001), pp. 200–208.
- ³⁶R. B. Marinenko, in *Standards for Electron Probe Microanalysis* (Plenum, New York 1991), pp. 251–260.
- ³⁷A. Bentien, M. Christensen, J. D. Bryan, A. Sanchez, S. Paschen, F. Steglich, G. D. Stucky, and B. B. Iversen, *Phys. Rev. B* **69**, 045107 (2004).